JOURNAL OF CATALYSIS 75, 207–218 (1982)

Effects of the Support in Fe_2O_3–MoO_3/Al_2O_3 Catalysts

M. CARBUCICCHIO

Gruppo Nazionale di Struttura della Materia del C.N.R., Istituto di Fisica, Università degli Studi di Parma, Parma, Italy

AND

F. TRIFIRÒ AND A. VACCARI

Istituto di Tecnologie Chimiche Speciali, Università degli Studi di Bologna, Italy

Received July 7, 1980; revised October 27, 1981

Diffuse reflectance, ESR and Mössbauer measurements were carried out on Fe_2O_3 and $Fe_2O_3 \cdot 4(MoO_3)$ supported on α- and γ-alumina before and after their interaction with methanol. These data were compared with the catalytic behaviour in the oxidation of methanol to formaldehyde in a fluidized bed reactor. For α-Al_2O_3-supported catalysts, $Fe_2(MoO_4)_3$ and Fe(III) dissolved within the lattice were detected. Also for γ-Al_2O_3-supported catalysts, two Fe(III)-containing compounds were found, namely, Fe(III) dissolved within the carrier and another Fe–Mo-containing compound which was considered to be either a surface Fe–Mo bilayer or a surface Fe–Al–Mo heteromolybdate. This latter compound is active only in dimethyl ether formation.

1. INTRODUCTION

Chemical characterization and study of the reactivity of the surfaces of many catalytic systems by spectroscopic techniques are often accomplished by using supports with high surface areas (*1–3*). From an industrial point of view, supported catalysts are of great interest (*4*) due to their mechanical strength, thermal and chemical stability, and resistance to abrasion.

In particular, iron molybdate presents a very low mechanical strength (*5*) and for this reason the oxidation of methanol is normally carried out in fixed bed reactors (*6*). By using a support it is possible to increase the catalyst strength. This allows one to utilize fluidized bed reactors for the industrial production of formaldehyde (*7*). However, previous investigations (*8–10*) demonstrated that reactions occur between the supported active species and carriers such as silica and alumina.

The aims of this paper are (i) to investigate the catalytic behaviour of $Fe_2O_3 \cdot 4(MoO_3)$ on α- and γ-Al_2O_3 in the oxidation of methanol in fluidized bed reactors and (ii) to obtain more information about the reactions occurring between the active species and the support. In order to achieve this objective reduction of the catalysts with methanol and reoxidation with air were carried out. The systems were characterized by diffuse reflectance, ESR, and Mössbauer measurements. For comparison, the measurements of $Fe(III)/Al_2O_3$ systems are also reported, for which many data are available in the literature (*11–20*).

2. EXPERIMENTAL

In order to obtain supports with different surface areas, alumina (Saint Gobain, 125 m^2/g) was calcined at 1100°C for different periods of time. In this way it is known that not only does the support area decrease but also the $\gamma \rightarrow \theta \rightarrow \alpha$ phase transition occurs in the alumina.

For BET measurements of surface area, a Carlo Erba sorptomatic apparatus with N_2 adsorption was used. The X-ray diffraction patterns of alumina were recorded by a Seifert spectrogoniometer using Cu$K\alpha$ radi-

0021-9517/82/060207-12$02.00/0

ation. Only the α phase was found for supports with areas $\leq 5\ m^2/g$.

Active component, 2.3% by weight, with stoichiometry $Fe_2O_3 \cdot 4(MoO_3)$ was supported on the carriers by impregnating $(NH_4)_6Mo_7O_{24} \cdot 4H_2O$, citric acid, and $Fe(NO_3)_3 \cdot 9H_2O$ according to Ref. (*8*). For comparison, 0.51% by weight of Fe_2O_3 was also supported on alumina by impregnating $Fe(NO_3)_3 \cdot 9H_2O$ and following the same treatment. The total amount of Fe(III) for all the samples was lower than the solubility limits for alumina.

In the following sections the samples will be labelled by indicating the supported species as FeMo or Fe and, in brackets, the surface area.

The catalytic activity was measured using a cylindrical fluidized bed reactor made of Pyrex with height h = 1000 mm and internal diameter d = 28 mm. The reactant was distributed from a porous disc with ~15-μm holes. The length of the bed was 450 mm and the linear velocity was v = 5.6 cm/s. The methanol concentration was 5.5% in air.

The diffuse reflectance spectra were obtained by a Perkin–Elmer model 124 spectrophotometer equipped with an integrator apparatus.

The ESR spectra were recorded at room temperature by a Varian E-104 X-band spectrometer equipped with conventional accessories.

The Mössbauer absorption spectra of the ^{57}Fe 14.4-keV γ radiation were measured by means of a constant-acceleration spectrometer and a source of 25 mCi ^{57}Co in Rh matrix. The spectra were fitted by superimposing a series of Lorentzian lines.

Both reducibility by methanol and reoxidizability by air of supported catalysts were analysed by measuring room-temperature Mössbauer, diffuse reflectance, and ESR spectra for samples which had been kept in a nitrogen–methanol stream (10% CH_3OH, total flow 6.21 ml/min) for 3 h at 320°C (reduction) and then kept in air for 7 h at 365°C (reoxidation). The treatment cell was directly connected by sidearms to the measurement cells, and the transfer of the catalysts was achieved at room temperature in a N_2 atmosphere, by rotation of the system.

3. RESULTS

Diffuse Reflectance Spectra

Figure 1 shows the diffuse reflectance spectra for (a) calcined FeMo[0.5], (b) Fe[5], (c) FeMo[5], (d) Fe[125], (e) FeMo[125], and (f) FeMo[125] reduced by methanol.

The spectrum of the FeMo[0.5] displays a sharp absorption at 440 nm characteristic of $Fe_2(MoO_4)_3$ (*21*).

Fe[5] and FeMo[5] (Figs. 1b and c) display an absorption quasi continuum from 580 nm to lower wavelengths, already attributed to the charge transfer band of Fe(III) (*19*). Similar but more intense absorption is shown by Fe[125]. This absorption is practically absent in FeMo[125].

The spectrum of FeMo[125] after interaction with methanol shows a large absorption in the entire visible region. The original spectrum is restored by oxygen treatment.

ESR Spectra

In Figs. 2a and c, are reported respectively the ESR spectra for FeMo[0.5] and FeMo[5]. For comparison, Fig. 2b shows the spectrum for Fe[5].

The multiline contribution to all these spectra can be attributed, according to Ref. (*20*), to Fe(III) dissolved in α-Al_2O_3 in trigonally distorted octahedral sites. The intense signal with g_{eff} = 2.0, observed only for FeMo[0.5] and FeMo[5] (Figs. 2a and c), is due to a condensed iron phase and can be attributed to $Fe_2(MoO_4)_3$ (*22*).

In Figs. 3a and b, are reported respectively the ESR spectra for calcined Fe[125] and FeMo[125]. The two spectra are very similar and show a broader signal at g_{eff} = 2.0, a sharp signal at g_{eff} = 4.3, and a final signal at $g_{eff} \simeq 10$.

In the spectrum obtained for FeMo[125]

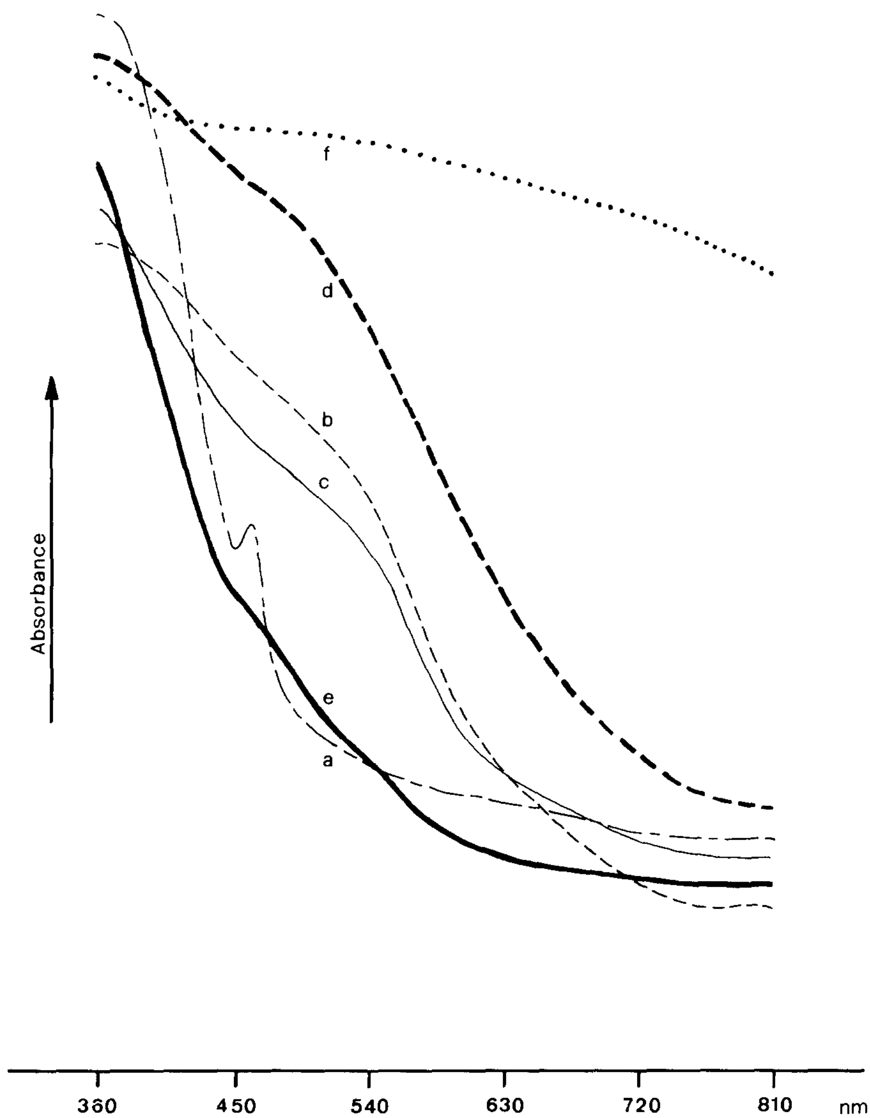

FIG. 1. Diffuse reflectance spectra: $Fe_2O_3 \cdot 4(MoO_3)$ on 0.5 m^2/g (a) and 5 m^2/g α-Al_2O_3 (c) and on 125 m^2/g γ-Al_2O_3 calcined (e) and reduced by methanol (f); Fe_2O_3 on 5 m^2/g α-Al_2O_3 (b) and 125 m^2/g γ-Al_2O_3 (d).

which had interacted with methanol (Fig. 3c) no remarkable change in the $g_{eff} = 4.3$ and $g_{eff} \simeq 10$ resonances is detectable, while the $g_{eff} = 2.0$ is masked by an additional very broad signal, not well identified. The sample reoxidation gives rise to an ESR spectrum similar to that of calcined FeMo[125] (Fig. 3b).

ESR spectra similar to those shown in Figs. 3a and b were already reported (*20*) for Fe(III) on γ-Al_2O_3 and attributed to Fe(III) with rhombically distorted site symmetry, dissolved in the lattice of γ-Al_2O_3.

Mössbauer Measurements

Figures 4a and b show the Mössbauer spectra for FeMo[0.5] and FeMo[5], respectively.

For FeMo[0.5] (Fig. 4a) the single line spectrum displays the same isomer shift

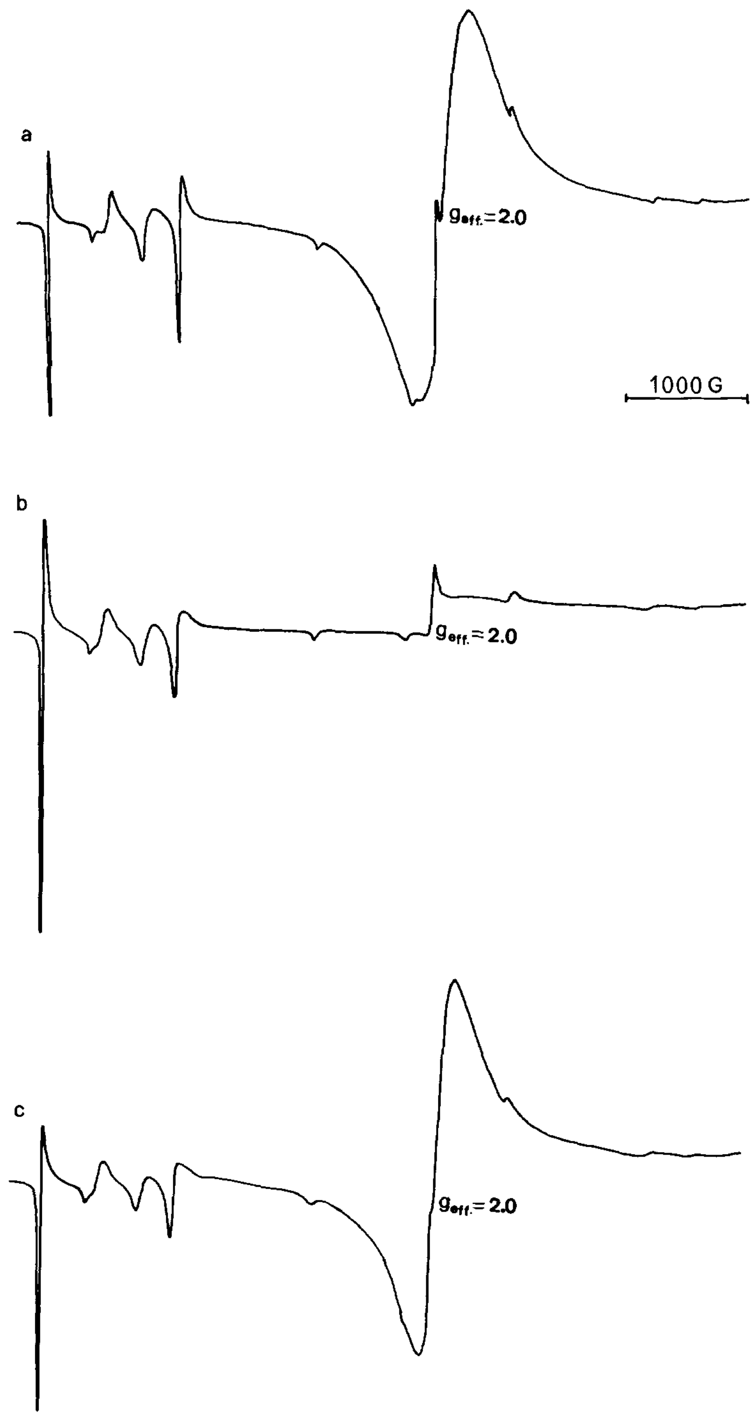

FIG. 2. ESR spectra: $Fe_2O_3 \cdot 4(MoO_3)$ on 0.5 m^2/g (a) and 5 m^2/g α-Al_2O_3 (c); Fe_2O_3 on 5 m^2/g α-Al_2O_3 (b).

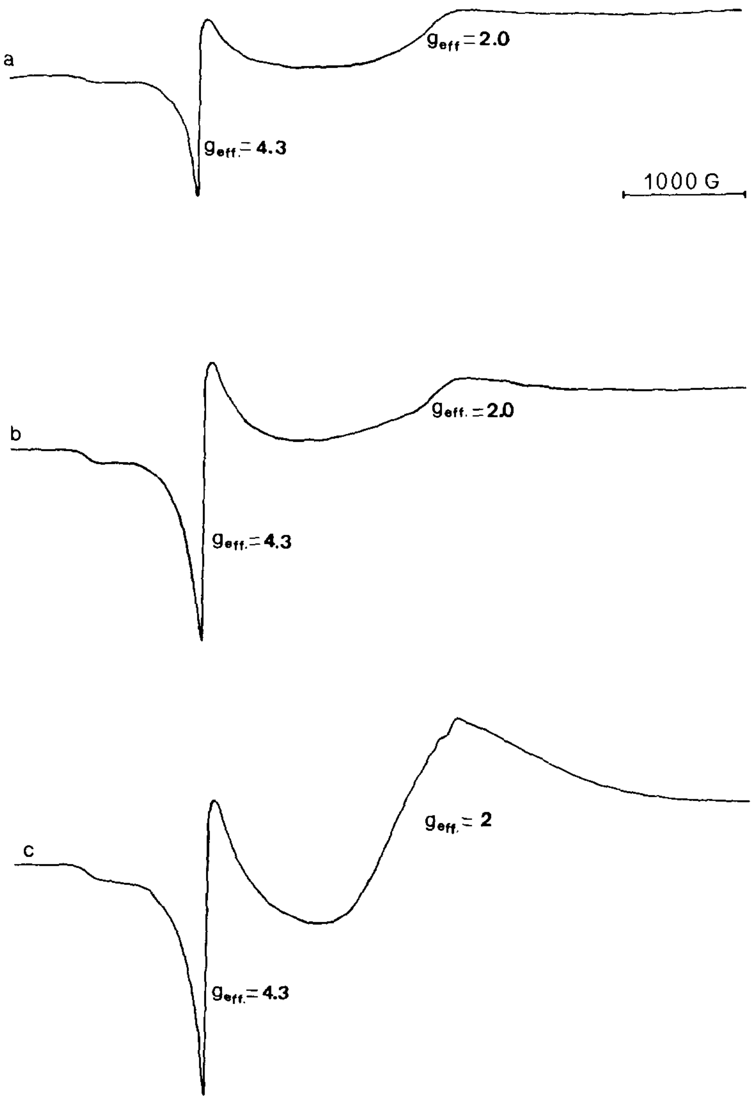

FIG. 3. ESR spectra: Fe_2O_3 on 125 m^2/g γ-Al_2O_3 (a); $Fe_2O_3 \cdot 4(MoO_3)$ on 125 m^2/g γ-Al_2O_3 calcined (b) and reduced by methanol (c).

and linewidth (Table 1) as those measured for $Fe_2(MoO_4)_3$ (*23*). By increasing the support area, the spectrum becomes broader (Fig. 4b).

Figure 4c shows the spectrum for FeMo[5] which had interacted with methanol under the same conditions which are known to give rise to complete reduction of $Fe_2(MoO_4)_3$ to β-$FeMoO_4$ (*23, 24*).

A good fit to the spectra measured for calcined and reduced FeMo[5] (Figs. 4b and c) was obtained in the first case by superimposing a single peak on a quadrupole doublet (δ) and, in the second case, by superimposing three quadrupolar doublets (δ, ϵ, and η). The Mössbauer parameters of all the spectral contributions are reported in Table 1.

The position of the single line contribution (Fig. 4b) is coincident with that of the single line spectrum due to pure $Fe_2(MoO_4)_3$. The linewidth, however, is greater.

The quadrupole splittings and isomer

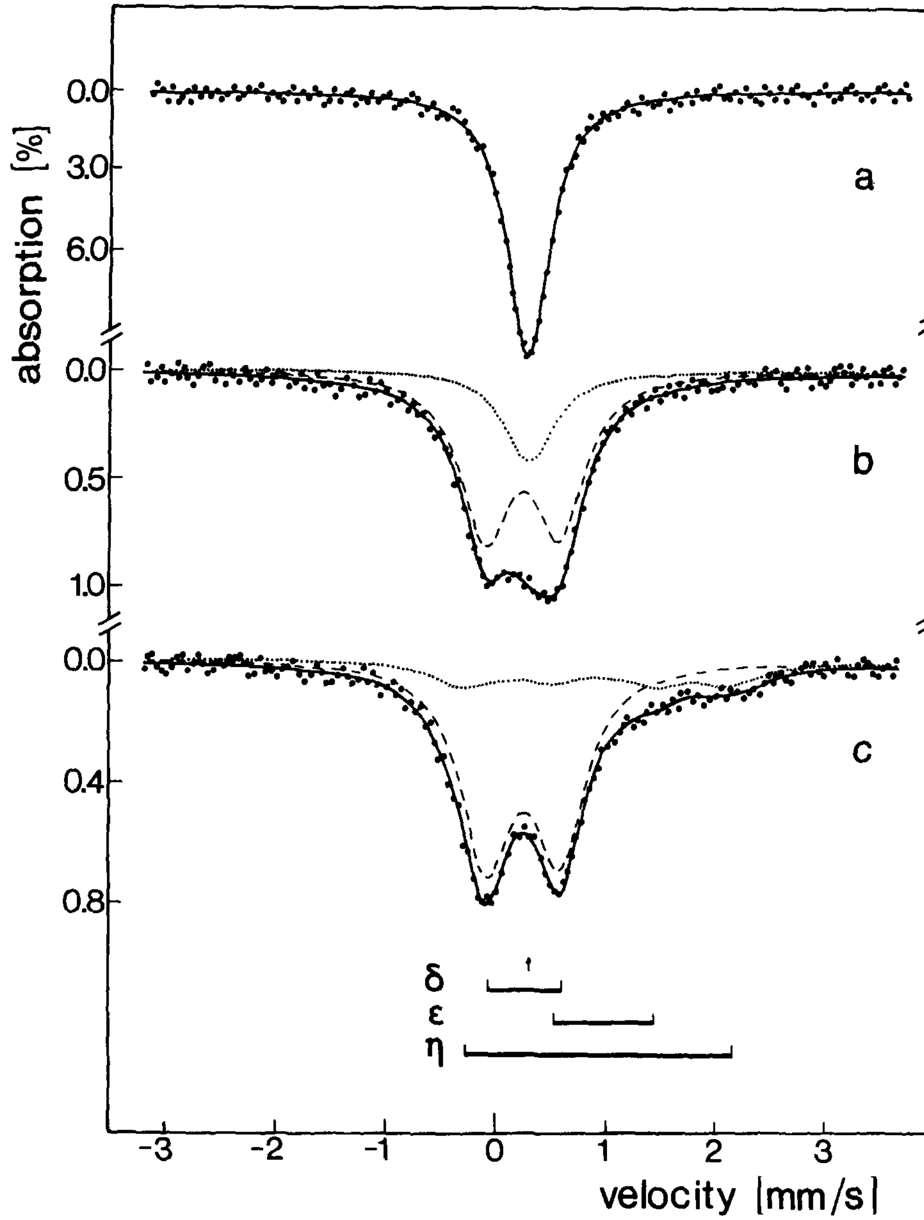

FIG. 4. Room-temperature Mössbauer spectra: $Fe_2O_3 \cdot 4(MoO_3)$ on 0.5 m^2/g (a) and 5 m^2/g α-Al_2O_3 calcined (b) and reduced by methanol (c). Zero velocity: ^{57}Fe in Rh.

shifts relative to ϵ and η doublets measured for the reduced sample (Fig. 4c), are coincident with those for the β-$FeMoO_4$ compound (*23*). The linewidths, however, are larger.

As for pure iron molybdate (*23*), the high-temperature interaction of the reduced sample (Fig. 4c) with air gives rise to a Mössbauer spectrum very similar to that measured before the reduction (Fig. 4b).

No differences in the δ doublet have been observed for the calcined and the reduced sample. Its Mössbauer parameters coincide with those measured for the Fe[5] double line spectrum (Table 1). Temperature-dependent Mössbauer measurements, as well

TABLE 1

Isomer Shifts Referred to Rh (IS), Quadrupole Splittings (QS), and Linewidths (Γ) (in mm/sec)

Sample	Single peak		Quadrupolar doublets																				
			δ			ε			η			κ			μ			ν			π		
	IS	Γ	IS	QS	Γ	IS	QS	Γ	IS	QS	Γ	IS	QS	Γ	IS	QS	Γ	IS	QS	Γ	IS	QS	Γ
2.3% $Fe_2O_3 \cdot 4(MoO_3)$ on 0.5 m^2/g α-Al_2O_3	0.30	0.49																					
2.3% $Fe_2O_3 \cdot 4(MoO_3)$ on 5 m^2/g α-Al_2O_3	0.31	0.58	0.25	0.68	0.56																		
2.3% $Fe_2O_e \cdot 4(MoO_3)$ on 5 m^2/g α-Al_2O_3 red			0.26	0.70	0.57	0.97	0.87	0.76	0.96	2.42	0.77												
β-$FeMoO_4$ (*23*)						0.99	0.90	0.40	0.94	2.44	0.42												
0.61% Fe_2O_3 on 5 m^2/g α-Al_2O_3			0.21	0.72	0.59																		
2.3% $Fe_2O_3 \cdot 4(MoO_3)$ (*9*) on 125 m^2/g γ-Al_2O_3												0.19	1.04	0.67	0.21	1.91	0.68						
2.3% $Fe_2O_3 \cdot 4(MoO_3)$ on 125 m^2/g γ-Al_2O_3 red												0.23	1.02	0.68				0.89	1.74	0.62	1.11	2.19	0.64
0.61% Fe_2O_3 on 125 m^2/g γ-Al_2O_3												0.21	0.99	0.70									

Note: The error for all the measured parameters is ±0.03 mm/s.

as the measurements we carried out for reduced and reoxidized FeMo[5] and Fe[5], suggest that this doublet is due to Fe(III) dissolved within the α-Al_2O_3 lattice (*26, 27*). It is worth noting that the above measurements, as compared with those reported in the literature (*25–30*), allow one to exclude the formation of α-Fe_2O_3, even if present in the form of very small particles. In particular Hobert and Arnold (*25*), who studied finely distributed iron oxides on the surface of various oxide carriers, showed that samples with very fine particles of ferric oxide yield mainly Fe^{2+}, and small amounts of metallic ferromagnetic iron, as products of reduction.

Figure 5a shows the spectrum for FeMo[125]. This spectrum can be inter-

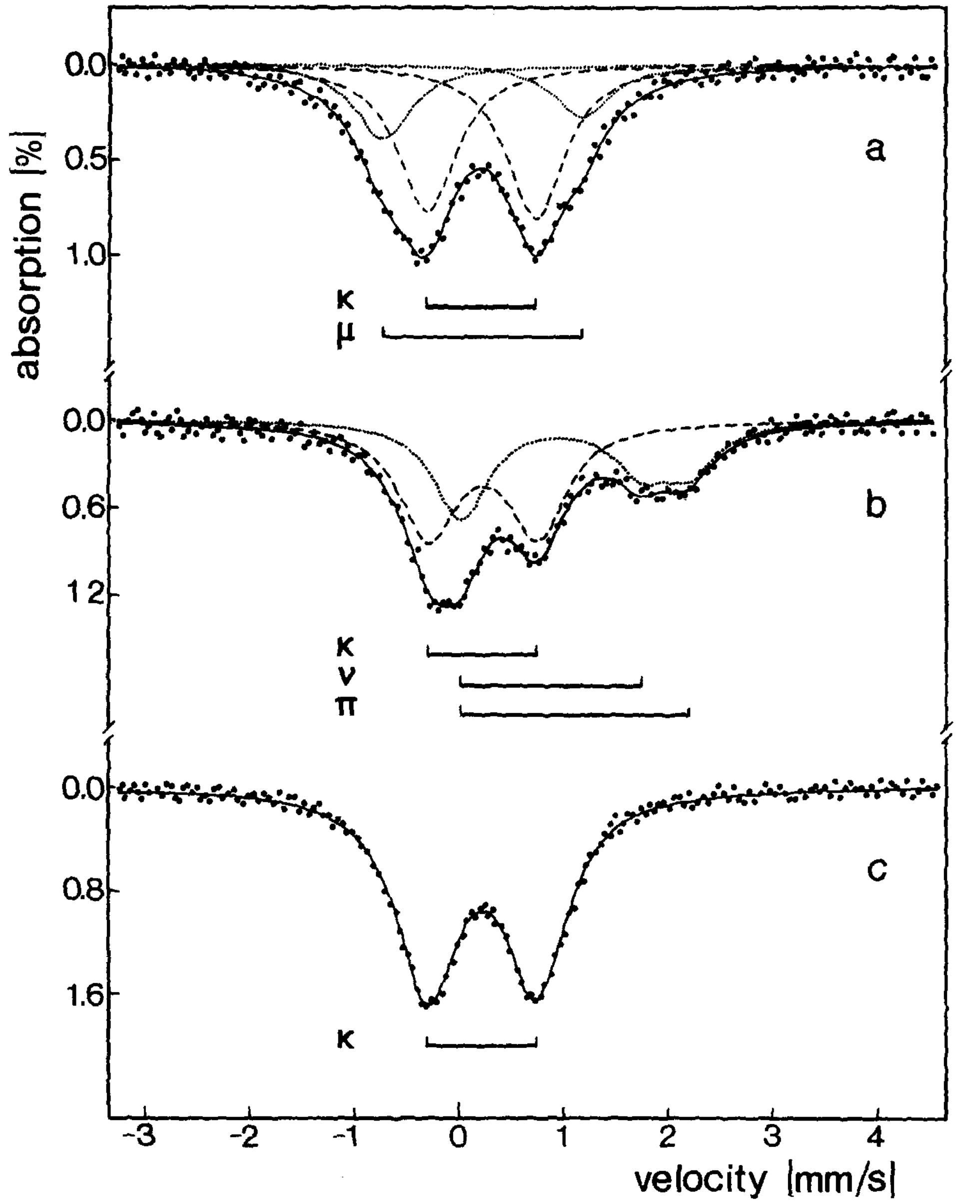

FIG. 5. Room-temperature Mössbauer spectra: $Fe_2O_3 \cdot 4(MoO_3)$ on 125 m^2/g γ-Al_2O_3 calcined (a) and reduced by methanol (b); Fe_2O_3 on 125 m^2/g γ-Al_2O_3 (c). Zero velocity: ^{57}Fe in Rh.

preted as being due to the superimposition of the two quadrupolar doublets indicated in the figure by the symbols κ and μ.

Figure 5b shows the spectrum for FeMo[125] after the methanol interaction. The experimental points were fitted by superimposing three quadrupole Lorentzian doublets (κ, ν, and π).

Figure 5c shows the spectrum measured for Fe[125]. This spectrum, fitted by two Lorentzian lines (Table 1), can be attributed to Fe(III) dissolved within the γ-Al_2O_3 lattice (*14, 15, 31*). Within experimental uncertainty, it coincides with the κ doublet which contributes to the spectra for calcined and reduced FeMo[125].

The μ quadrupolar doublet transforms into ν and π doublets as a consequence of the methanol interaction. These doublets can be attributed to two kinds of Fe(II) ions. Their parameters (Table 1), however, are not comparable with those measured for β-$FeMoO_4$, in accordance with the fact that $Fe_2(MoO_4)_3$ was not present in the oxidized compound.

The spectrum measured for the reduced FeMo[125] (Fig. 5b) which was kept in air at 365°C for 7 h is very similar to that measured before the methanol interaction (Fig. 5a).

Catalytic Measurements

In Table 2 the conversion and the yields for FeMo[0.5], FeMo[5], and FeMo[125] catalysts for different reaction temperatures are reported. For comparison, the catalytic data for γ-Al_2O_3 125 m^2/g are also listed. By increasing the catalyst surface area, both selectivity and activity undergo a remarkable change.

FeMo[0.5] shows appreciable activity only for the higher tested temperatures with a high selectivity for formaldehyde. This behaviour is very similar to that found for unsupported $Fe_2(MoO_4)_3$ (*23*). In the case of FeMo[5], the selectivity of CH_2O is strongly decreased. CO, CO_2, dimethyl ether (DME), and methyl formate (MeFo) were found as by-products. FeMo[125] gives rise as main product to DME while CH_2O is absent. As by-products, there are only CO and CO_2 present in very small quantities. It is interesting to note that on γ-

TABLE 2

Activity and Selectivity Data in the Oxidation of Methanol Using a Fluidized Bed Reactor

Catalyst	Temperature (°C)	Conversion (%)	CO (%)	CO_2 (%)	DME[a] (%)	CH_2O (%)	MeFo[b] (%)
2.3% $Fe_2O_3 \cdot 4(MoO_3)$ on 0.5 m^2/g α-Al_2O_3	220	18.0	0.09	0.01	—	0.89	—
	250	45.0	0.22	0.02	—	2.23	—
	280	70.0	0.33	0.02	—	3.50	—
2.3% $Fe_2O_3 \cdot 4(MoO_3)$ on 5 m^2/g α-Al_2O_3	190	26.2	—	—	0.25	1.12	0.07
	220	51.3	0.09	0.01	0.32	2.12	0.28
	250	77.5	0.55	0.05	0.28	3.08	0.30
	280	96.5	1.82	0.10	0.01	3.34	0.04
2.3% $Fe_2O_3 \cdot 4(MoO_3)$ on 125 m^2/g γ-Al_2O_3	190	85.3	0.10	0.01	4.58	—	—
	220	89.6	0.38	0.02	4.53	—	—
	250	94.0	0.62	0.03	4.52	—	—
125 m^2/g γ-Al_2O_3	310	84.0	4.24	0.38	—	—	—

Note. Experimental conditions: length of bed 450 mm, linear velocity v = 5.6 cm/s, methanol concentration 5.5% in air.

[a] DME = Dimethyl ether.

[b] MeFo = Methyl formate.

Al_2O_3 125 m^2/g the methanol oxidizes to CO and CO_2 exclusively.

4. DISCUSSION

α-Al_2O_3-Supported Catalysts

The value of selectivity to CH_2O obtained with FeMo[0.5] was 90% at the highest level of conversion and is comparable with that obtained for pure (*23*) and silica-supported iron molybdate (*8*, *10*). On increasing the surface area, a benefit in conversion was observed, but the value of selectivity fell to 80%. New by-products, such as DME and MeFo, and higher amounts of CO and CO_2 were observed. It is interesting to note that on SiO_2 with higher surface areas (15 and 39 m^2/g) only a slight decrease in activity and selectivity was observed (*8*).

This comparison leads to the following considerations:

(i) the decrease in selectivity cannot be attributed simply to the increase in porosity;

(ii) SiO_2 and α-Al_2O_3 react in different ways with $Fe_2O_3 \cdot 4(MoO_3)$.

Both Mössbauer and ESR measurements revealed the existence of two different Fe(III) species.

The first species is not reducible at the temperature at which the catalysts are active in the methanol oxidation and probably it does not participate in the catalytic oxidation process. It can eventually modify the acid–base sites of the support influencing the formation of DME. This species gives rise to the doublet δ in the Mössbauer spectra and to the multiline contribution in the ESR spectra and can be identified as Fe(III) dissolved in the α-Al_2O_3 lattice.

The second species is reducible by methanol in a reversible way and it was not present in Fe[5]. This species which gives rise to the strong signal at g_{eff} = 2.0 in the ESR spectra and to the single line contribution in the Mössbauer spectra can be attributed to $Fe_2(MoO_4)_3$.

The product of the reduction of this species, as can be deduced from the Mössbauer analysis, is β-$FeMoO_4$, by analogy with the behaviour of unsupported $Fe_2(MoO_4)_3$. The formation of all the oxidized products of methanol can therefore be attributed to the presence of iron molybdate.

By increasing the surface area of the support from 0.5 to 5 m^2/g we observed an increase of the activity, notwithstanding the decrease of the amount of the $Fe_2(MoO_4)_3$. This may be due to the increase of the surface area of the active species.

The decrease in selectivity observed by increasing the support area must, however, be attributed to some modification of the active species. The presence of broad Mössbauer lines suggests a distribution of iron sites with slightly different quadrupole interactions.

γ-Al_2O_3-Supported Catalysts

FeMo[125] no longer showed the property of oxidation of methanol to formaldehyde. Dimethyl ether was the main product with small amounts of CO and CO_2.

Also for FeMo[125], two types of Fe(III) were found: the first one, not reducible by methanol, gives rise to the κ quadrupolar doublet in the Mössbauer spectra and to the signals at g_{eff} = 2.0, g_{eff} = 4.3, and $g_{eff} \simeq 10$ in the ESR spectra. Therefore, it was identified to be Fe(III) dissolved in the γ-alumina lattice.

The existence of a compound containing another Fe(III) species is deduced from the presence of the μ quadrupolar doublet in the Mössbauer spectrum of calcined FeMo[125] (Fig. 5a), not found for Fe[125] (Fig. 5c). Mørup *et al.* (*15*) have not observed this second compound on Fe–Mo supported on γ-Al_2O_3. This can be due to the different method of impregnation and to the different amount of Fe–Mo supported on the γ-Al_2O_3.

The fact that ESR measurements of calcined FeMo[125] do not reveal characteristic signals for this compound can be explained, according to Ref. (*32*), by assuming that the resonance pattern of this Fe(III) is very broad and weak.

The diffuse reflectance spectrum of calcined FeMo[125] (Fig. 1e) as compared with that of Fe[125] (Fig. 1d) displays a strong decrease of the quasi-continuum absorption below 580 nm. The decrease of this absorption suggests that the molybdenum destroys the charge transfer between iron–oxygen–iron surface species. This could be due either to the formation of a surface layer of MoO_3 or to the formation of a surface iron–molybdenum-containing compound. For $Fe_2O_3 \cdot 4(MoO_3)$ supported on silica with higher surface area, the residual activity and selectivity in CH_2O were attributed to the formation of free MoO_3 (*8, 10*). The absence of formaldehyde in the oxidation of methanol with FeMo[125] therefore allows one to exclude the presence of a surface layer of MoO_3.

Moreover, the formation of dimethyl ether, attributable to acid–base centers at the catalyst surface, suggests that, by supporting $Fe_2O_3 \cdot 4(MoO_3)$, the surface of the γ-alumina must be modified, as pure γ-alumina is active in the total methanol oxidation.

All these data, together with the data obtained after reduction, suggest that a reducible and reversibly reoxidizable compound, contining Fe(III) and Mo(VI), is present at the surface of the FeMo[125].

Analogies may exist between the Fe–Mo–Al_2O_3 and Co–Mo–Al_2O_3 systems. Regarding this latter system, the existence of interactions between the surface and Co(II) and Mo(VI) was reported by many authors (*33–37*), interactions which do not lead to the formation of definite molybdate. According to Delmon and co-workers (*37, 38*), these interactions can be connected with the formation of a Co–Mo bilayer.

The evidence reported in this paper about the presence of a surface compound containing Fe and Mo supports the hypothesis of the formation of either a Fe–Mo bilayer or a Fe–Al–Mo heteromolybdate on the surface of γ-alumina.

ACKNOWLEDGMENT

This work was supported by the National Research Council (CNR) of Italy.

REFERENCES

1. GAGER, H. M., AND HOBSON, M. C., JR., *Catal. Rev. Sci.* **11,** 117 (1975).
2. SUZDALEV, I. P., FIRSOVA, A. A., AND MARGOLIS, L. YA., *Kinet. Katal.* **14,** 1341 (1973).
3. LEFTIN, H. P., AND HOBSON, M. C., *in* "Advances in Catalysis and Related Subjects," Vol. 14, p. 118. Academic Press, New York, 1963.
4. THOMAS, J. M., AND THOMAS, W. J., "Introduction to the Principles of Heterogeneous Catalysis." Academic Press, New York, 1967.
5. ALESSANDRINI, G., CAIRATI, L., FORZATTI, P., VILLA, P. L., AND TRIFIRÒ, F., *J. Less Common Met.* **54,** 373 (1977).
6. PERNICONE, N., *J. Less Common Met.* **36,** 289 (1974).
7. CAIRATI, L., FORZATTI, P., PASQUON, I., AND TRIFIRÒ, F., *Ind. Eng. Chem. Des. Dev.* **19,** 561 (1980).
8. CAIRATI, L., CARBUCICCHIO, M., RUGGERI, O., AND TRIFIRÒ, F., *in* "Preparation of Catalysts II" (B. Delmon, P. Grange, P. Jacobs, and G. Poncelet, Eds.), p. 279. Elsevier, Amsterdam, 1979.
9. CARBUCICCHIO, M., *J. Chem. Phys.* **70,** 784 (1979).
10. CARBUCICCHIO, M., AND TRIFIRÒ, F., *J. Catal.* **62,** 13 (1980).
11. WERTHEIM, G. K., AND REMEIKA, J. P., *Phys. Lett.* **10,** 14 (1964).
12. BHIDE, V. G., AND DATE, S. K., *Phys. Rev.* **172,** 345 (1968).
13. HOBSON, M. C., JR., AND GAGER, H. M., *in* "Proceedings, 4th International Congress on Catalysis, Moscow, 1968," Vol. II, p. 28. Akadémiai Kiadó, Budapest, 1971.
14. WERTHEIM, G. K., AND BUCHANAN, D. N. E., *in* "Proceedings, 2nd Int. Mössbauer Conf., Saclay, 1961," p. 130. Wiley, New York, 1962.
15. MØRUP, S., CLAUSEN, B. S., AND TOPSØE, H., *J. Phys. (Paris)* **40,** C2-88 (1979).
16. YOSHIOKA, T., KOEZUKA, J., AND IKOMA, H., *J. Catal.* **16,** 264 (1970).
17. GARTEN, R. L., AND OLLIS, D. F., *J. Catal.* **35,** 232 (1974).
18. DUMESIC, J. A., AND TOPSØE, H., *in* "Advances in Catalysis and Related Subjects," Vol. 26, p. 121. Academic Press, New York, 1977.
19. KLIER, K., *Catal. Rev.* **1,** 207 (1967).
20. POTT, G. T., AND MCNICHOL, B. D., *Discuss. Faraday Soc.* **52,** 121 (1971).

21. VILLA, P. L., SZABO, A., TRIFIRÒ, F., AND CARBUCICCHIO, M., *J. Catal.* **47**, 122 (1977).
22. BORESKOV, G. K., KOLOVERTNOV, G. D., KEFELI, L. M., PLAYSOVA, L. M., KARAKCHIEV, L. G., MASTIKHIN, V. N., POPOV, B. I., DZISKO, V. A., AND TARASOVA, D. V., *Kinet. Katal.* **7**, 125 (1966).
23. CARBUCICCHIO, M., AND TRIFIRÒ, F., *J. Catal.* **45**, 77 (1976).
24. CARBUCICCHIO, M., TRIFIRÒ, F., AND VILLA, P. L., *J. Phys.* (*Paris*) **37**, C6-253 (1976).
25. HOBERT, H., AND ARNOLD, D., *in* "Proceedings, Int. Conf. Appl. Mössbauer Effect, Tihany, 1969," p. 325. Akâdemiai Kiadó, Budapest, 1971.
26. HOBSON, M. C., JR., AND GAGER, H. M., *J. Catal.* **16**, 254 (1970).
27. JANOT, CH., AND DELCROIX, P., *J. Phys.* (*Paris*) **35**, C6-557 (1974).
28. CONSTABARIS, G., LINDQUIST, R. H., AND KÜNDIG, W., *Appl. Phys. Lett.* **7**, 59 (1965).
29. VAN DER KRAAN, A. M., *Phys. Status Solidi A* **18**, 215 (1973).
30. KRUPYANSKII, YU. F., AND SUZDALEV, I. P., *Sov. Phys. JETP* **38**, 359 (1974).
31. TOPSØE, H., AND MØRUP, S., *in* "Proceedings, Int. Conf. Mössbauer Spectroscopy, Krakow 1975," Vol. 1, p. 305. Akademia Górniczo-Hutnicza, Krakow, 1975.
32. CASTNER, T., NEWELL, G. S., HOLTON, W. C., AND SLICHTER, C. P., *J. Chem. Phys.* **32**, 668 (1960).
33. LO JACONO, M., CIMINO, A., AND SCHUIT, G. C. A., *Gazz. Chim. Ital.* **103**, 1281 (1973).
34. GRIMBLOT, J., AND BONNELLE, J. P., *J. Electron Spectrosc.* **9**, 449 (1976).
35. MONÉ, R., *in* "Preparation of Catalysts" (B. Delmon, P. A. Jacobs, and G. Poncelet, Eds.), p. 381. Elsevier, Amsterdam, 1976.
36. TRIFIRÒ, F., *Gazz. Chim. Ital.* **64**, 377 (1974).
37. DELMON, B., AND HOUALLA, M., *in* "Preparation of Catalysts II" (B. Delmon, P. Grange, P. Jacobs, and G. Poncelet, Eds.), p. 439. Elsevier, Amsterdam, 1979.
38. APECETCHE, M. A., AND DELMON, B., *React. Kinet. Catal. Lett.* **12**, 385 (1979).